International Immunology, Vol. 18, No. 1, pp. 59–68
doi:10.1093/intimm/dxh349

Expression of aberrant forms of CD22 on B lymphocytes in *Cd22*^{a} lupus-prone mice affects ligand binding

Lars Nitschke[1], Frédéric Lajaunias[2], Thomas Moll[2], Liza Ho[2], Eduardo Martinez-Soria[2], Shuichi Kikuchi[2], Marie-Laure Santiago-Raber[2], Carolin Dix[1], R. Michael E. Parkhouse[3] and **Shozo Izui[2]**

[1]Department of Genetics, University of Erlangen, 91058 Erlangen, Germany
[2]Department of Pathology and Immunology, University Medical Center, CMU, 1211 Geneva 4, Switzerland
[3]Gulbenkian Institute for Science, Oeiras, Portugal

Keywords: Systemic lupus erythematosus, Siglec, CD22 ligand, Autoimmune diseases

Abstract

CD22 functions primarily as a negative regulator of B-cell receptor signaling. The *Cd22*^{a} allele has been proposed as a candidate allele for murine systemic lupus erythematosus. In this study, we explored the possible expression of aberrant forms of CD22, which differ in the N-terminal sequences constituting the ligand-binding site due to synthesis of abnormally processed *Cd22* mRNA, in several *Cd22*^{a} mouse strains, including C57BL/6 *Cd22* congenic mice. The staining pattern of splenic B cells obtained with CY34 anti-CD22 mAb, which was expected to bind poorly to the aberrant CD22, was more heterogeneous in *Cd22*^{a} mice than in *Cd22*^{b} mice. Moreover, CD22 detected on B cells of *Cd22*^{a} mice was expressed more weakly and as a smaller-sized protein, compared with *Cd22*^{b} mice. Significantly, analysis with a synthetic CD22 ligand demonstrated that *Cd22*^{a} mice carried a larger proportion of CD22 that was not bound by *cis* ligands on the B-cell surface than *Cd22*^{b} mice. Finally, the study of C57BL/6 *Cd22* congenic mice revealed that *Cd22*^{a} B cells displayed a phenotype reminiscent of constitutively activated B cells (reduced surface IgM expression and augmented MHC class II expression), as reported for B cells expressing a mutant CD22 lacking the ligand-binding domain. Our demonstration that *Cd22*^{a} B cells express aberrant forms of CD22, which can potentially deregulate B-cell signaling because of their decreased ligand-binding capacity, provides further support for *Cd22*^{a} as a potential candidate allele for murine systemic lupus erythematosus.

Introduction

CD22 is a B cell-specific member of the Ig superfamily with seven Ig-like domains, which functions as an adhesion receptor recognizing α2,6-linked sialic acid (2,6Sia)-bearing glycans on target cells, and as a co-receptor for B-cell receptor (BCR) (1). Upon BCR cross-linking, CD22 is rapidly tyrosine phosphorylated on its cytoplasmic tail, which results in recruitment and activation of SH-2 phosphotyrosine phosphatase (SHP-1), thereby negatively regulating BCR signaling (2). Furthermore, the finding that CD22-deficient B cells exhibit a greatly enhanced and prolonged Ca^{2+} signal after BCR stimulation (3–6) indicates that CD22 functions primarily as a negative regulator of BCR signaling by controlling the threshold of BCR-mediated signal transduction. CD22-deficient B cells also show higher tyrosine phosphorylation of several signaling molecules which positively regulate Ca^{2+} mobilization (1). One mechanism by which CD22 regulates Ca^{2+} signaling has recently been uncovered: CD22 attenuates calcium efflux by activating a plasma membrane calcium-ATPase, the activation of which requires tyrosine phosphorylation of CD22 and SHP-1 (7).

CD22 is a member of the sialic acid-binding Ig-like lectin (Siglec) family of adhesion receptors, which bind specifically to sialic acids in characteristic linkages (8). CD22 has a specificity for 2,6Sia, a common structure on N-linked glycans that are abundantly expressed on the surface of many cells (9, 10). CD22 binds to 2,6Sia with its first Ig-like domain (11, 12). The affinity of CD22 for sialic acids is very low and does not differ greatly for several sialylated proteins, suggesting that it is just the presence and density of the carbohydrate, but not the protein backbone, that determines ligand binding

Correspondence to: S. Izui; E-mail: shozo.izui@medecine.unige.ch

Received 1 July 2005, *accepted* 6 October 2005

Transmitting editor: M. Miyasaka

Advance Access publication 15 November 2005

(13). It has been shown that CD22 is constitutively bound to ligands in *cis*, i.e. to ligands on the same cellular surface, on the majority of both human and mouse B cells (14–16). These *cis* interactions seem to regulate the inhibitory signaling function of CD22, because when they were blocked in established B-cell lines, lower tyrosine phosphorylation of CD22 and higher Ca^{2+} signaling after BCR activation were observed (17, 18). Recently, a CD22 knock-in mouse with a mutated CD22 ligand-binding domain confirmed the important biological role of 2,6Sia binding for CD22 (19). However, enhanced Ca^{2+} signaling was not observed in this knockin mouse.

The CD22^a protein carries a 6-amino-acid deletion and 8-amino-acid substitutions in the first Ig-like domain, as compared with CD22^b (20). In addition, we have demonstrated that the *Cd22^a* gene contains a short interspersed nucleotide element insertion in the second intron (21). As a consequence, *Cd22^a* B cells synthesize abnormally processed *Cd22* mRNA, which contains insertions of ~20–120 nucleotides between exons 2 and 3, and/or deletions of ~100–190 nucleotides in exon 4 encoding the first Ig-like domain of CD22. Thus, it has been speculated that *Cd22^a* B cells could express aberrant forms of CD22, which differ in the N-terminal sequences constituting the ligand-binding site (17, 18, 22). We explored this possibility by assessing the binding to B cells of two different anti-CD22 mAb, CY34 and NIM-R6, which apparently recognize an epitope present in the first or fourth Ig-like domain, respectively (22, 23), and by analyzing the expression of aberrant CD22 protein from *Cd22^a* mice by Western blot. In addition, we determined the binding capacity of B cells from different mouse strains bearing either the *Cd22^a* or *Cd22^b* allele for a synthetic ligand containing 2,6Sia. Our results demonstrate that a larger proportion of CD22 is not bound by *cis* ligand on *Cd22^a* B cells, as compared with *Cd22^b* B cells, indicating the expression of aberrant forms of CD22 with a decreased ligand-binding capacity in *Cd22^a* mice.

Methods

Mice

C57BL/6 (B6; *Cd22^b*), BALB/c (*Cd22^b*), C3H (*Cd22^b*), DBA/2 (*Cd22^a*), NZB (*Cd22^a*) and NZW (*Cd22^a*) mice were purchased from the Jackson Laboratories, Bar Harbor, ME, USA. CD22$^{-/-}$ mice with a pure B6 background were developed as described previously (6). B6 mice bearing the *Cd22^a* allele were generated by backcross procedures using marker-assisted selection, as described previously (24).

Flow cytometric analysis

Flow cytometry was performed using two-color staining of lymphocytes, and analyzed with a FACSCalibur (BD Biosciences, San Jose, CA, USA). The following antibodies and reagents were used: FITC-labeled NIM-R6 rat anti-CD22 (20), FITC-labeled CY34 rat anti-CD22 (25), FITC-labeled rat IgG, polyclonal rabbit anti-CD22 antibodies, raised against Ig-like domains 1–3 of the CD22^b protein by immunizing rabbits with a CD22 domains 1–3-Fc fusion protein, and affinity purified (the expression construct was generously provided by A. van der Merwe, Oxford and P. Crocker, Dundee), FITC-labeled goat anti-rabbit IgG, FITC- or PE-labeled RA3-6B2 rat anti-B220, PE-labeled 53-7.3 rat anti-CD5, biotinylated 7G6 rat anti-CD21, FITC-labeled LO-MM9 rat anti-mouse IgM and FITC-labeled Y-3P anti-I-A^b.

Western blot analysis

Total lysates of spleen cells from 2-month-old B6, BALB/c, DBA/2 and NZB mice were separated by a 6% SDS-PAGE and transferred to Immobilon-P transfer membrane (Millipore, Volketswil, Switzerland) with a semi-dry blotting apparatus (BioRad, Glattbrugg, Switzerland). After 2 h of blocking at room temperature in TTBS (10 mM Tris–HCl, pH 7.4, 100 mM NaCl and 0.05% Tween 20) containing 5% low-fat, dry milk powder (TTBS-MP), the membranes were incubated with polyclonal rabbit anti-CD22 antibodies in TTBS-MP overnight at 4°C. Polyclonal rabbit anti-LYN antibodies (Santa Cruz Biotechnology, Heidelberg, Germany) were used as a loading control. Thoroughly washed membranes were incubated with HRP-conjugated goat anti-rabbit IgG (BioRad) for 1 h at room temperature. Chemiluminescence development was carried out with the enhanced chemiluminescence reagents (Amersham Bioscience, Dübendorf, Switzerland) and the membranes were exposed to HyperFilm ECL (Amersham).

Cell culture

A total of 2×10^6 spleen cells from a pool of 2-month-old mice were incubated in 1 ml of DMEM containing 10% FCS in Falcon 24-well plates in the presence of 25 μg ml^{-1} LPS for 48 h. Then, the expression of CD22 on B cells was determined by flow cytometric analysis. B cells were purified from spleen by adherence of macrophages to plastic plates for 1 h at 37°C and subsequent treatment with anti-Thy-1.2 (AT-83) mAb in the presence of rabbit complement. The purity of B cells, as documented by cytofluorometric analysis, was superior to 95%. B-cell proliferative responses were determined by incubating 2×10^5 spleen cells from B6 mice with different concentrations of rat b7-6 anti-mouse IgM mAb, rat FGK45 anti-mouse CD40 mAb or LPS in a total volume of 200 μl DMEM containing 10% FCS. Cultures were pulsed with 1 μCi of [^{3}H]thymidine for the final 6 h of 3-day culture, harvested and counted for radioactivity.

Staining of cells with a synthetic CD22 ligand

Preparation and use of the synthetic probe, *N*-glycolylneuramic acid–galactose–*N*-acetylglucosamine–streptavidin–alkaline phosphatase (NeuGcα2,6Gal–SAAP), have been described in detail elsewhere (16). NeuGcα2,6Gal–SAAP consists of the sialoside NeuGcα2,6Galα1,4GlcNAc–biotin, bound to streptavidin–alkaline phosphatase, which is then FITC-labeled. The probe used for the experiments here is a new preparation which gives a higher degree of background staining with CD22$^{-/-}$ B cells, than previously (16). For staining, single-cell suspensions were prepared from total spleen. Prior to FACS analysis, all cells were depleted of erythrocytes by lysis with hypotonic Gey's solution. Sialidase treatment was performed with 0.1 U ml^{-1} neuraminidase of *Arthrobacter ureafaciens* (Roche Applied Science, Mannheim, Germany) for 1 h at 37°C in PBS-0.1% BSA. A total of 1×10^5 to 2×10^5

erythrocyte-depleted splenic cells were first stained with anti-B220 mAb. Staining with FITC-labeled NeuGcα2,6Gal–SAAP was performed by incubating the cells with the probe for 45 min on ice. Flow cytometry was performed as described above.

Ca^{2+} mobilization measurements

Spleen cells were loaded with Indo-1 (Molecular Probes, Eugene, OR, USA), as described (17, 18), and stained with FITC-labeled anti-B220 mAb. Splenocytes were then stimulated with 10, 30 or 90 μg ml^{-1} of b7-6 anti-IgM mAb at 37°C, and increases in intracellular free Ca^{2+} in B220$^+$ B cells were measured in real time with the use of a FACSVantage (BD Biosciences). The recorded files were transferred to FlowJo software (Tree Star, Ashland, OR, USA), and the median of each sample was calculated.

Results

Heterogeneous staining pattern of Cd22^a B cells with CY34, but homogeneous staining pattern with NIM-R6

When splenic B cells from 2-month-old DBA/2 (*Cd22^a*), NZB (*Cd22^a*), NZW (*Cd22^a*), B6 (*Cd22^b*) and BALB/c (*Cd22^b*) mice were stained with FITC-labeled CY34 mAb, the intensity of surface staining on *Cd22^a* B220$^+$ B cells, gated using PE-labeled anti-B220 mAb, was lower than that of *Cd22^b* B cells (Fig. 1). Moreover, it was striking to see that the staining pattern of B cells with the CY34 mAb was more heterogeneous in the three strains of mice bearing the *Cd22^a* allele than that of *Cd22^b* B6 and BALB/c mice (Fig. 1). In contrast, splenic B cells from the three different *Cd22^a* strains exhibited a homogeneous staining pattern by FITC-labeled NIM-R6 mAb, similar to that observed in *Cd22^b* mice. Notably, the intensity of NIM-R6 staining on *Cd22^b* B cells was significantly higher than that observed on *Cd22^a* B cells, although the differences were relatively small ($P < 0.005$). These results suggested that, unlike CD22 expressed by mice carrying the *Cd22^b* allele, CD22 molecules on B cells from mice bearing the *Cd22^a* allele were more heterogeneous because of differences in their N-terminal region. This is consistent with the finding that *Cd22^a* B cells express multiple forms of *Cd22* mRNA transcripts having highly variable N-terminal sequences coding for the first Ig-like domain.

Expression of smaller-sized CD22 proteins in Cd22^a B cells than in Cd22^b B cells

To further address whether aberrant forms of CD22 protein are expressed in B cells of *Cd22^a* mice, splenic B cells were analyzed with a polyclonal rabbit anti-CD22 antibody raised against murine CD22^b (Ig-like domains 1–3). Western blot analysis revealed that CD22 migrated as a slightly smaller-sized protein in B cells from *Cd22^a* mice (DBA/2 and NZB) than CD22 detected in B cells from *Cd22^b* mice (B6 and BALB/c) (Fig. 2A). We also noted lower intensities of the CD22 bands in *Cd22^a* mice. This was confirmed by flow cytometric analysis, showing that the intensity of rabbit anti-CD22 staining on the surface of *Cd22^a* B cells was significantly lower than that on the surface of *Cd22^b* B cells (Fig. 2B). These differences could be explained by two reasons: a lower expression of CD22 protein by *Cd22^a* mice and a lower reactivity to CD22^a of the rabbit anti-CD22 antibodies used in this analysis because these antibodies were raised against a polypeptide spanning the first three Ig-like domains in which substantial amino-acid substitutions were identified between the CD22^a and CD22^b proteins (22, 23).

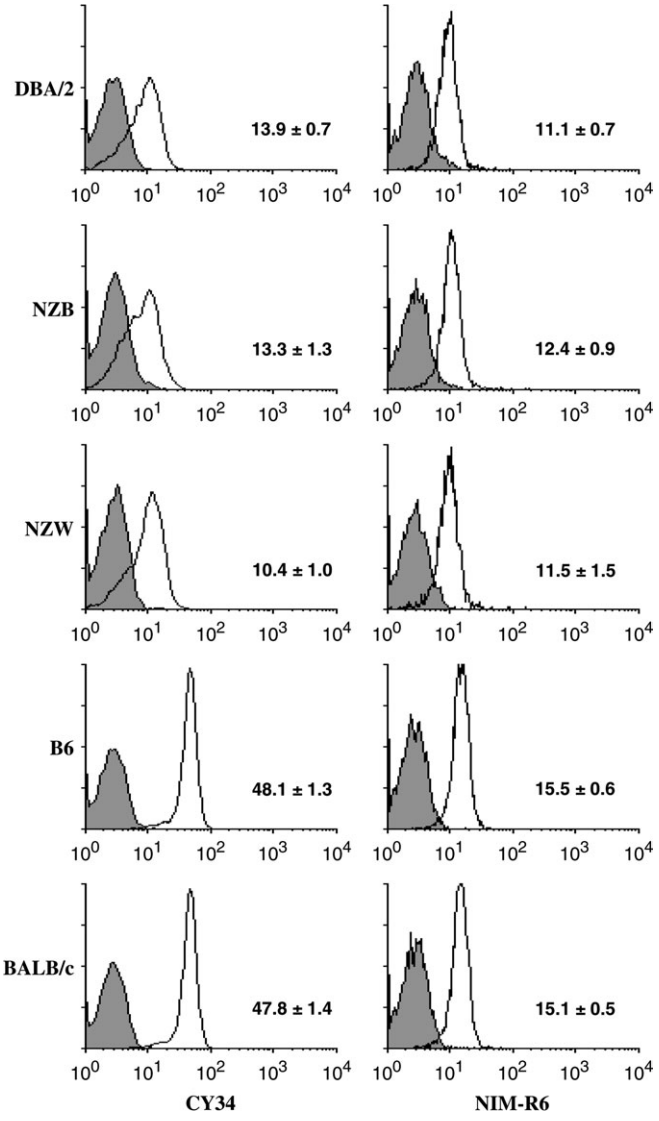

Fig. 1. Heterogeneous staining pattern of *Cd22^a* B cells with CY34 mAb, but homogeneous staining pattern with NIM-R6 mAb. Spleen cells from 2-month-old DBA/2 (*Cd22^a*), NZB (*Cd22^a*), NZW (*Cd22^a*), B6 (*Cd22^b*) and BALB/c (*Cd22^b*) mice were stained with either FITC-labeled CY34 or NIM-R6 anti-CD22 mAb. Histograms show representative results of CY34 and NIM-R6 staining on B220$^+$ B cells obtained from five to seven individual mice. Mean fluorescence intensities (±SD) of CY34 and NIM-R6 staining of each strain of mice are indicated. Differences between *Cd22^a* and *Cd22^b* mice for both stainings were significant ($P < 0.005$ by the Wilcoxon two-sample test). Shaded histograms indicate the background staining of B cells with FITC-labeled control rat IgG conjugates, except for B6 mice, where shaded histograms indicate the staining of B cells from CD22$^{-/-}$ B6 mice with FITC-labeled CY34 or NIM-R6 anti-CD22 mAb.

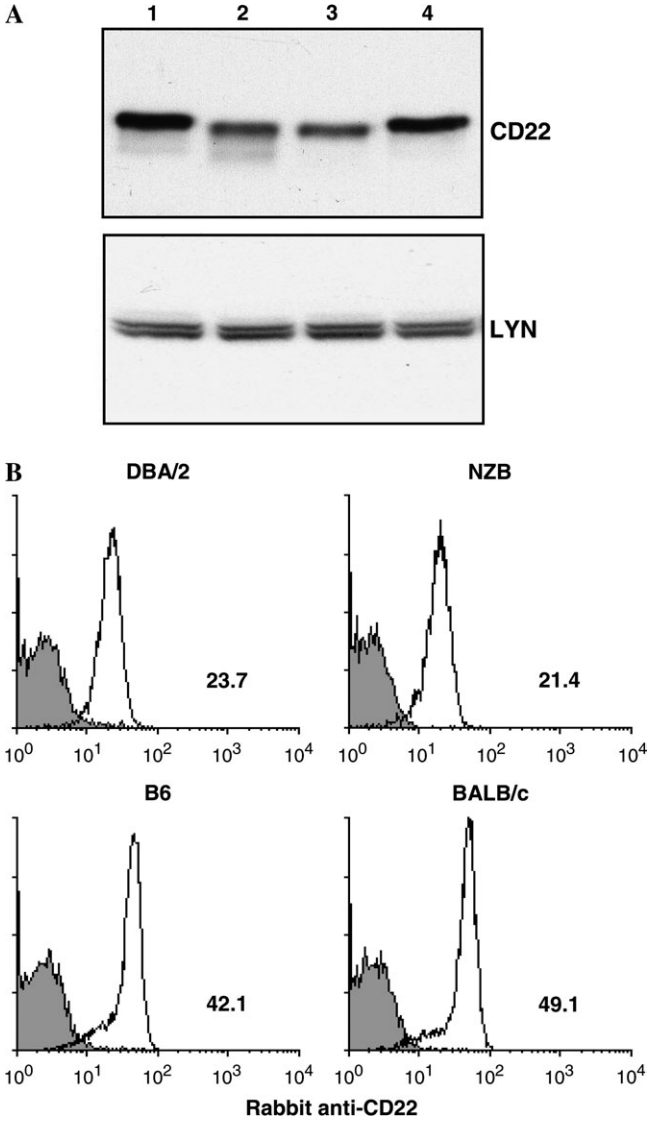

Fig. 2. Expression of smaller-sized CD22 proteins in *Cd22^{a}* B cells than *Cd22^{b}* B cells. (A) Western blot analysis of CD22 protein expression in *Cd22^{a}* (DBA/2 and NZB) and *Cd22^{b}* (B6 and BALB/c) B cells. Total lysates of spleen cells from 2-month-old mice were analyzed by SDS-PAGE with subsequent immunoblot analysis with rabbit anti-CD22 or anti-LYN antibodies. 1: B6, 2: DBA/2, 3: NZB, 4: BALB/c. One representative result from two independent experiments is shown. (B) Spleen cells from the indicated mice were stained with rabbit anti-CD22 antibodies, followed by FITC-labeled goat anti-rabbit IgG. Histograms show representative results of anti-CD22 staining on B220^{+} B cells, with mean fluorescence intensities from three individual mice. Shaded histograms indicate background staining of B cells with FITC-labeled goat anti-rabbit IgG conjugates alone.

Limited up-regulation of CD22 bearing the CY34 epitope in Cd22^{a} B cells stimulated with LPS

We have previously observed, by staining with NIM-R6 mAb, that B cells of NZW (*Cd22^{a}*) mice up-regulated CD22 less efficiently after activation with LPS in the presence of IL-4 than those of B6 (*Cd22^{b}*) mice (21). To further define the expression of aberrant and intact CD22 in *Cd22^{a}* B cells, we compared the level of CD22 molecules detectable by CY34 or NIM-R6 mAb after incubation of spleen cells with LPS. After 48 h of LPS stimulation, splenic B cells from *Cd22^{a}* (DBA/2, NZB and NZW) mice displayed increases in CD22 levels detectable by NIM-R6 mAb, though less than those observed in *Cd22^{b}* (B6 and BALB/c) mice (Fig. 3). In contrast, the level of CD22 recognized by CY34 mAb was barely increased in *Cd22^{a}* B cells, as compared with *Cd22^{b}* B cells, probably due to the presence of CD22 molecules with an aberrant first Ig-like domain that were poorly detected by CY34 mAb. Significantly, after LPS stimulation of splenic B cells from NZW and NZB mice, we observed a substantial increase in the number of B cells expressing aberrant CD22, which was very poorly recognized by the CY34 mAb. It should be mentioned that the CY34^{lo} subset did not express CD5 at a significant level (data not shown), indicating that these were not B-1 cells present in high numbers in NZB mice (26). Since an expansion of the CY34^{lo} subset was not observed in LPS-stimulated spleen cells from non-autoimmune DBA/2 mice, this finding is likely related to the particular genetic background of autoimmune-prone NZW and NZB mice. All these data support the expression of aberrant forms of CD22 on the surface of *Cd22^{a}* B cells.

Increased binding by Cd22^{a} B cells to a synthetic CD22 ligand

Since the CD22^{a} protein carries mutations in exon 4 coding for the ligand-binding first Ig-like domain (20), we tested whether sialic acid binding is affected by these mutations. To examine the ligand-binding capacity of CD22^{a} *in situ* on the surface of B cells, we used a synthetic probe, NeuGcα2,6Gal–SAAP which carries 2,6Sia coupled as an oligomer to streptavidin. As previously described (16), most CD22 on the surface of B cells of B6 mice (*Cd22^{b}*) was 'masked' by binding to endogenous ligands in *cis* and therefore could not be stained by the probe NeuGcα2,6Gal–SAAP (Fig. 4A). However, there was a sub-population (~10%) of B cells with 'unmasked' CD22, which could be stained with NeuGcα2,6Gal–SAAP. Next, we compared the NeuGcα2,6Gal–SAAP binding with B cells from three strains of *Cd22^{b}* mice with three strains of *Cd22^{a}* mice. The *Cd22^{b}* strains B6, BALB/c and C3H showed on average 10–11% of B cells which were stained with the probe (Fig. 4A). In contrast, for the *Cd22^{a}* strains NZB, NZW and DBA/2 probe binding to B cells was significantly increased (1.5- to 1.8-fold). This indicated a higher degree of unmasked, i.e. not *cis*-bound, CD22 in the *Cd22^{a}* strains. Not all probe binding was CD22 specific, as can be seen by staining of B cells from CD22-deficient mice. Residual binding of NeuGcα2,6Gal–SAAP to CD22$^{-/-}$ B cells could be due to other Siglecs expressed, or could be unspecific binding.

Then, we tested the capacity of CD22^{a} and CD22^{b} to bind the synthetic probe after removal of *cis* ligands from the surface of B cells by sialidase treatment. After a treatment with sialidase, B cells from all CD22-sufficient mice showed increased binding of the NeuGcα2,6Gal–SAAP probe (Fig. 4B). However, under the sialidase treatment conditions used, there was still a difference between B cells from *Cd22^{b}* and *Cd22^{a}* mice, and B cells from *Cd22^{a}* mice showed a clearer shift toward probe-stained cells. As expected, the majority of

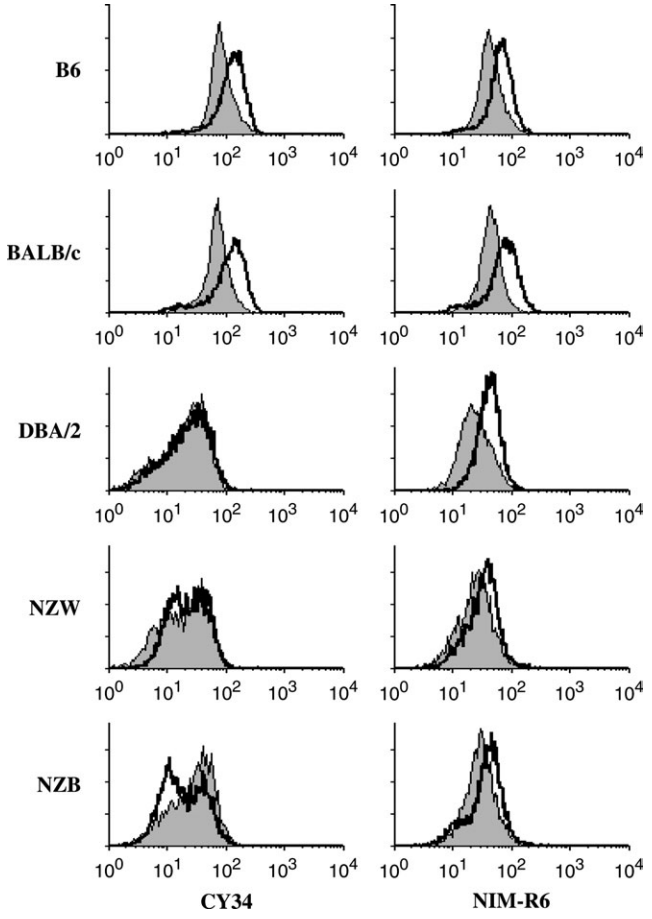

Fig. 3. Altered activation-induced up-regulation of surface CD22 on splenic B cells from *Cd22^a* and *Cd22^b* mice. Spleen cells from 2-month-old *Cd22^a* (DBA/2, NZB and NZW) and *Cd22^b* (B6 and BALB/c) mice were incubated with 25 μg ml^{-1} of LPS for 48 h, and the expression levels of CD22 were assessed using FITC-labeled CY34 and NIM-R6 anti-CD22 mAb. Fluorescence intensities on stimulated (dark lines) and unstimulated (shaded) B220$^+$ B cells are shown. Representative results of three independent experiments are shown. Note a lack of up-regulation of CD22 detectable by CY34 mAb on LPS-stimulated B cells from *Cd22^a* (DBA/2, NZB and NZW) mice, and a significant expansion of the CY34^{lo} B-cell population in LPS-stimulated B cells from NZW and NZB mice. Although we noted some variations in LPS-induced B-cell proliferative responses, as determined by specific uptake of [^{3}H]thymidine, among various strains of mice (mean counts per minute ± 1 SD of three mice: DBA/2, 77 618 ± 9934; NZB, 82 798 ± 6338; NZW, 62 054 ± 10 418; B6, 83 218 ± 10 472; BALB/c, 50 027 ± 4058), no consistent differences were observed between *Cd22^a* and *Cd22^b* strains of mice.

CD22$^{-/-}$ B cells still failed to bind the probe after this treatment (Fig. 4B). These results indicate that not all 2,6Sia-containing CD22 ligands on CD22^b-expressing cells can be removed by sialidase treatment as easily as on CD22^a-expressing cells, suggesting that the former are less accessible. It should, however, be mentioned that *Cd22^a* B cells from NZB, NZW and DBA/2 mice did not show any significant differences in Ca^{2+} influx following BCR cross-linking with b7-6 anti-IgM mAb at any dose tested, as compared with *Cd22^b* B cells from B6, BALB/c and C3H mice (data not shown).

Defective expression of CD22 in B cells from B6 Cd22^a congenic mice

In order to exclude that the observed differences between *Cd22^a* and *Cd22^b* mice are due to unspecific strain background effects, B6 *Cd22^a* congenic mice were produced by backcross procedures and analyzed for the staining of splenic B cells with different anti-CD22 antibodies in comparison with that of *Cd22^b* B cells from conventional B6 mice. As observed in different strains of *Cd22^a* and *Cd22^b* mice, B6 *Cd22^a* B cells displayed weak and heterogeneous staining with CY34 mAb, and less strong staining with NIM-R6 mAb and polyclonal rabbit anti-CD22 antibodies, as compared with conventional B6 *Cd22^b* B cells (Fig. 5A). Moreover, Western blot analysis confirmed the expression of a smaller-sized CD22 protein in B6 *Cd22^a* B cells than in *Cd22^b* B cells (Fig. 5B). Furthermore, the binding study with synthetic NeuGcα2,6Gal–SAAP probe on untreated and sialidase-treated B cells demonstrated the presence of a larger proportion of unmasked CD22 on B6 *Cd22^a* B cells than on B6 *Cd22^b* B cells ($P < 0.05$; Fig. 6). Notably, the analysis of B-cell subsets in spleen by staining with anti-IgM and anti-CD21 mAb revealed that percentages of transitional 1 (T1; CD21$^-$IgM^{hi}), T2 and marginal zone (CD21^{hi}IgM^{hi}), and follicular (CD21^{int}IgM^{int}) B cells in B6 *Cd22^a* mice (means ± SD of three mice: T1, 6.6 ± 0.4%; T2 + marginal zone, 5.3 ± 0.7%; follicular, 45.1 ± 1.9%) were essentially identical to those from B6 *Cd22^b* mice (T1: 7.2 ± 1.1%; T2 + marginal zone: 6.4 ± 0.9%; follicular: 43.2 ± 0.2%). These data argued against the possibility that an imbalance in splenic B-cell subsets accounted for the higher unmasking of CD22 in *Cd22^a* mice.

Activated phenotype of B cells from B6 Cd22^a congenic mice

Studies with B cells expressing a mutant CD22 lacking the ligand-binding domain displayed a phenotype of constitutively activated B cells, as documented by reduced expression of IgM and increased expression of MHC class II on the surface of mature B cells (19). Therefore, we determined expression levels of surface IgM and MHC class II I-A molecules on splenic B cells from B6 *Cd22^a* mice in comparison with those on *Cd22^b* B cells. *Cd22^a* B cells were found to express significantly less surface IgM (mean fluorescence intensity: 59.9 ± 2.0) and more MHC class II I-A (172.0 ± 5.7) than B cells from *Cd22^b* counterparts (IgM, 65.6 ± 0.6; I-A, 151.1 ± 8.1; Fig. 7A).

It has also been reported that anti-IgM- and anti-CD40-induced B-cell proliferative responses were substantially reduced and modestly augmented, respectively, in mice expressing the mutant CD22 (19). Although we did not observe measurable differences in B-cell proliferative responses after stimulation with anti-CD40 mAb or LPS, BCR-induced proliferation after treatment with anti-IgM mAb was substantially reduced in *Cd22^a* B cells, compared with that of *Cd22^b* B cells (Fig. 7B). Despite significant reduced proliferative responses, *Cd22^a* B cells had Ca^{2+} mobilization comparable to that of *Cd22^b* B cells after stimulation with anti-IgM mAb (Fig. 7C), consistent with the results obtained with B cells expressing the mutant CD22 (19).

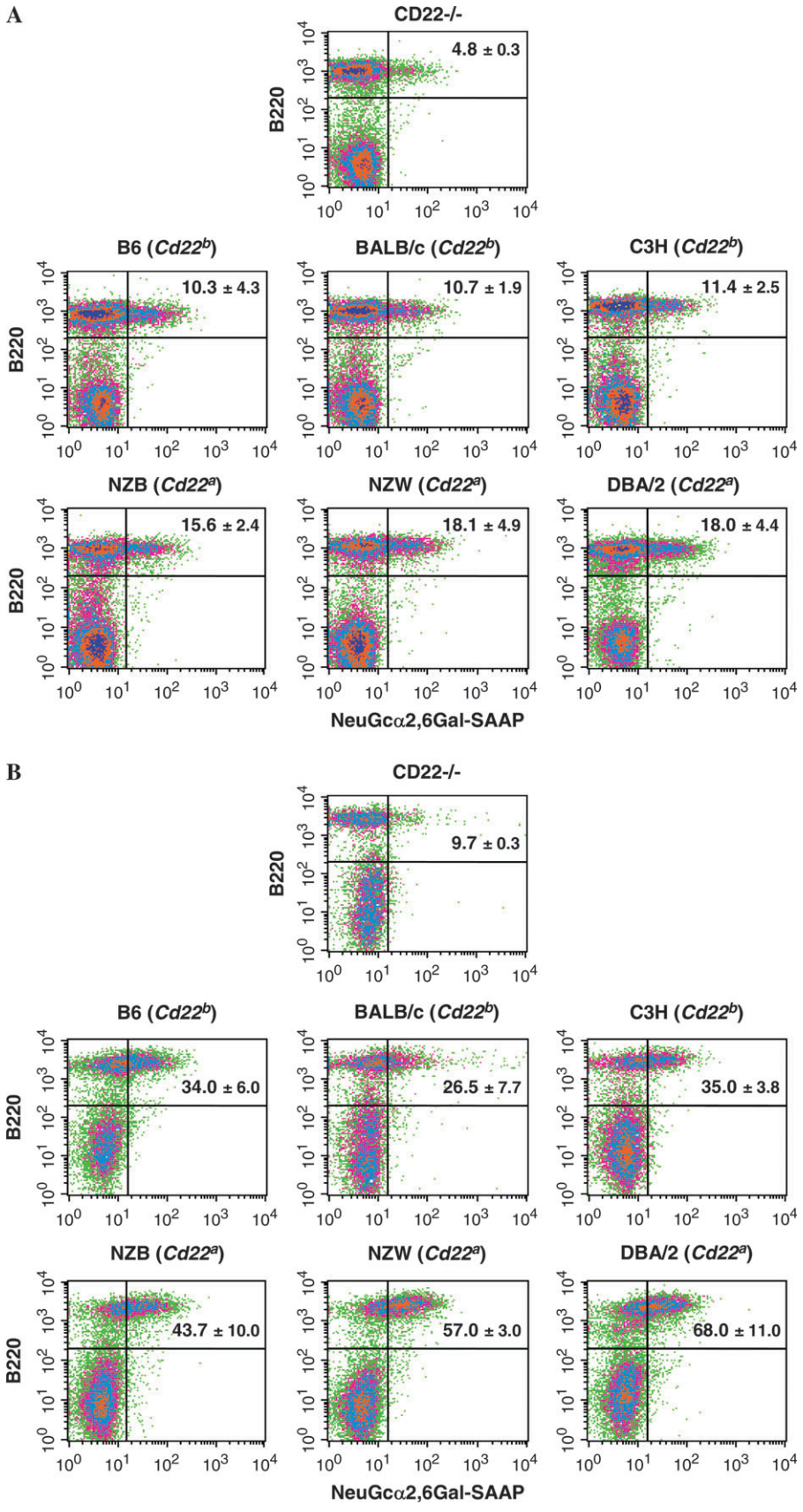
A
CD22-/-
4.8 ± 0.3
B6 (Cd22b)
10.3 ± 4.3
BALB/c (Cd22b)
10.7 ± 1.9
C3H (Cd22b)
11.4 ± 2.5
NZB (Cd22a)
15.6 ± 2.4
NZW (Cd22a)
18.1 ± 4.9
DBA/2 (Cd22a)
18.0 ± 4.4
B220
NeuGcα2,6Gal-SAAP
B
CD22-/-
9.7 ± 0.3
B6 (Cd22b)
34.0 ± 6.0
BALB/c (Cd22b)
26.5 ± 7.7
C3H (Cd22b)
35.0 ± 3.8
NZB (Cd22a)
43.7 ± 10.0
NZW (Cd22a)
57.0 ± 3.0
DBA/2 (Cd22a)
68.0 ± 11.0
B220
NeuGcα2,6Gal-SAAP

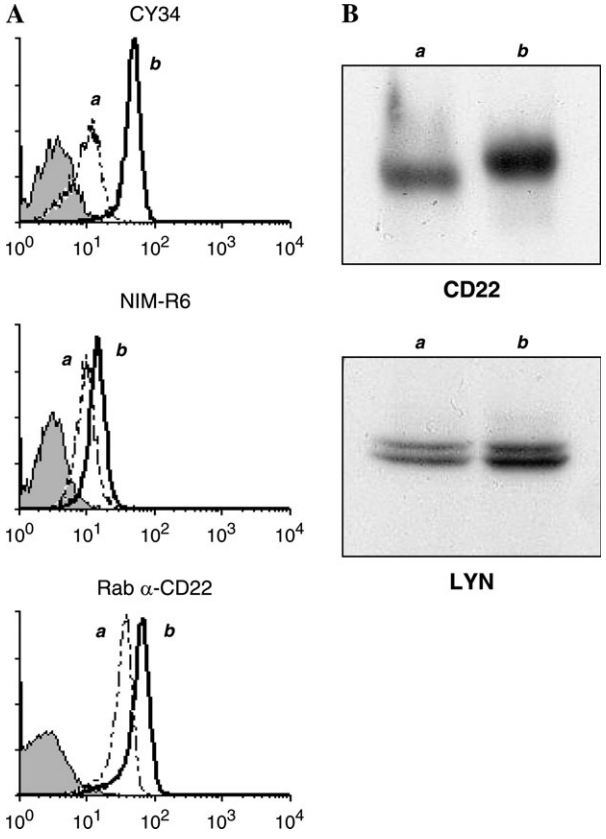

Fig. 5. Defective expression of CD22 in B cells from B6 *Cd22^a* congenic mice. (A) Spleen cells from 2-month-old *Cd22^a* and *Cd22^b* B6 mice were stained with CY34, NIM-R6 or rabbit anti-CD22 antibodies. Histograms show representative results of anti-CD22 staining on B220$^+$ B cells obtained from three individual mice (a, *Cd22^a*; b, *Cd22^b*). Shaded histograms indicate the background staining of B cells with FITC-labeled control conjugates alone. (B) Western blot analysis of CD22 protein expression in B6 *Cd22^a* and *Cd22^b* B cells. Total lysates of splenic cells from 2-month-old mice were analyzed by SDS-PAGE with subsequent immunoblot analysis with rabbit anti-CD22 or anti-LYN antibodies (a, *Cd22^a*; b, *Cd22^b*).

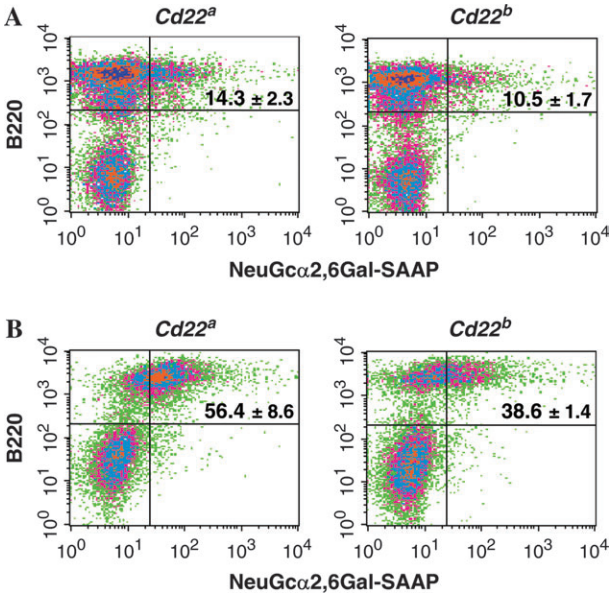

Fig. 6. Higher proportion of B cells bearing unmasked CD22 in B6 *Cd22^a* mice than in B6 *Cd22^b* mice. (A) Untreated splenocytes of 2-month-old *Cd22^a* and *Cd22^b* B6 mice were stained with PE-labeled anti-B220 and FITC-labeled NeuGcα2,6Gal–SAAP. Mean percentages (±1 SD of three mice) of B220$^+$ B cells that bind NeuGcα2,6Gal–SAAP (upper right quadrant) are indicated. (B) Splenocytes were pre-treated with sialidase to remove sialic acids from the cellular surface and then stained. The proportion of probe-bound cells after sialidase treatment was higher in *Cd22^a* than in *Cd22^b* mice, as shown by mean percentages (±1 SD) in upper right quadrants.

Discussion

We explored the possible expression of aberrant forms of CD22 on B cells from several *Cd22^a* mouse strains, including *Cd22^a* congenic C57BL/6 mice, by surface staining with CY34 and NIM-R6 anti-CD22 mAb, which recognize distinct epitopes of CD22, by Western blot, and by use of a synthetic CD22 ligand. Our data support the notion that *Cd22^a* B cells express aberrant forms of CD22 molecule that differ in the N-terminal region constituting the ligand-binding site for 2,6Sia-bearing glycans, as compared with CD22^b molecules. The analysis with a synthetic CD22 ligand revealed that CD22 protein from *Cd22^a* mice is less bound to endogenous ligands on the B-cell surface than their counterpart from *Cd22^b* strains, indicating a decreased ligand-binding capacity of CD22^a protein. This was further supported by the analysis of B6 *Cd22* congenic mice, which revealed that *Cd22^a* B cells displayed a phenotype reminiscent of constitutively activated B cells, as characterized by reduced surface IgM expression and augmented MHC class II expression, similar to that reported for B cells expressing a mutant CD22 lacking the ligand-binding domain (19).

The full-length CD22^a protein carries a 6-amino-acid deletion plus several point mutations in the first Ig-like domain, in comparison to the CD22^b protein (20). These mutations map to the C′ and C″ β-strands of one β-sheet, as can be deduced

Fig. 4. Higher proportion of B cells bearing unmasked CD22 in *Cd22^a* mice than in *Cd22^b* mice. (A) Untreated splenocytes of *Cd22^a* (NZB, NZW and DBA/2) and *Cd22^b* (B6, BALB/c and C3H) mice were stained with PE-labeled anti-B220 and FITC-labeled NeuGcα2,6Gal–SAAP. This probe detects CD22 molecules, which are not bound by endogenous ligands, i.e. unmasked CD22. Mean percentages (±1 SD) of B220$^+$ B cells that bind NeuGcα2,6Gal–SAAP (upper right quadrant) are indicated. Significance by Student's *t*-test ($n = 3$): NZB versus B6: $P < 0.05$; NZW versus B6: $P < 0.01$; DBA/2 versus B6: $P < 0.01$. Similar statistically significant differences were obtained when *Cd22^a* mice were compared with BALB/c and C3H mice. (B) Splenocytes were pre-treated with sialidase to remove sialic acids from the cellular surface and then stained. The proportion of probe-bound B cells after sialidase treatment was higher in *Cd22^a* than in *Cd22^b* mice, as shown by mean percentages (±1 SD) in upper right quadrants. Significance by Student's *t*-test ($n = 3$): NZB versus B6, BALB/c, C3H: not significant; NZW versus B6, BALB/c, C3H: $P < 0.01$; DBA/2 versus B6, BALB/c, C3H: $P < 0.01$. This was also corroborated by the mean fluorescence intensities of all B220$^+$ cells: B6 CD22$^{-/-}$: 5, B6: 13, BALB/c: 10, C3H: 11, NZB: 18, NZW: 22, DBA/2: 17. One representative result of three independent experiments is shown.

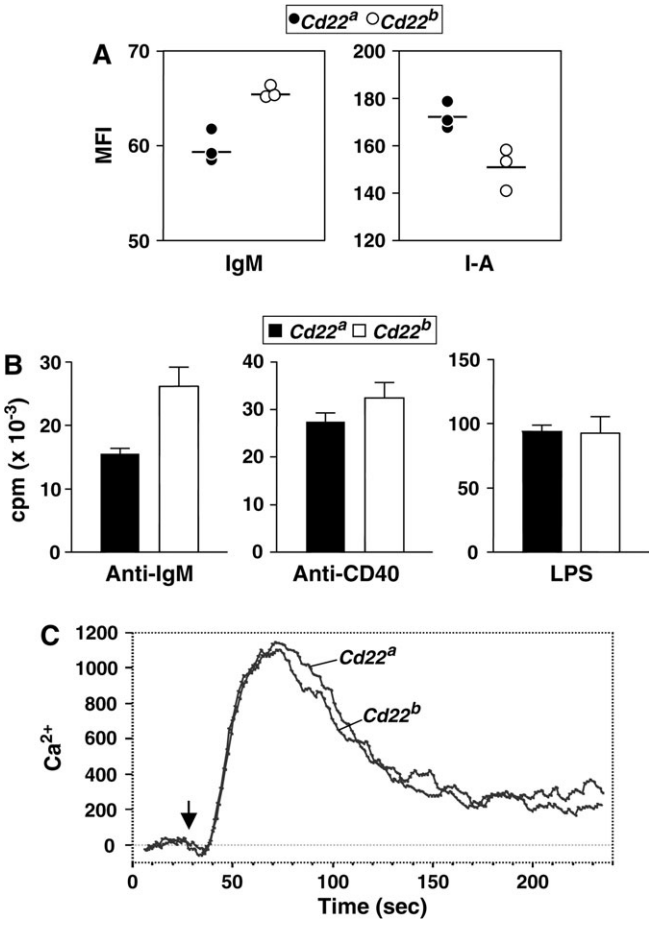

Fig. 7. B-cell phenotypes and B-cell proliferative and Ca^{2+} flux responses in B6 *Cd22^a* and *Cd22^b* congenic mice. (A) Spleen cells from 2-month-old B6 *Cd22^a* and *Cd22^b* mice were stained with a combination of anti-B220, anti-IgM and anti-I-A^b mAb. Results are expressed as mean fluoresence intensity obtained with anti-IgM and anti-I-A staining of $B220^+$ B cells. Each symbol represents an individual *Cd22^a* and *Cd22^b* mice, and mean values are indicated by horizontal lines. Significance by Student's *t*-test: IgM: $P < 0.01$; I-A: $P < 0.05$. (B) Splenic B-cell proliferative responses following stimulation with 25 μg ml^{-1} of b7-6 anti-IgM mAb, FGK45 anti-CD40 mAb or LPS in B6 *Cd22^a* and *Cd22^b* mice. Results are expressed as counts per minute of [^{3}H]thymidine ([^{3}H]Tdr) incorporation (means of three mice ±1 SD). Background uptake of [^{3}H]Tdr was 1109 ± 70 for *Cd22^a* B cells and 979 ± 47 for *Cd22^b* B cells. Significance by Student's *t*-test: anti-IgM, $P < 0.05$; anti-CD40 and LPS, not significant. (C) Spleen cells were loaded with Indo-1, stained with FITC-labeled anti-B220 mAb and then stimulated with 30 μg ml^{-1} of b7-6 anti-IgM mAb at 37°C. Increases in intracellular free Ca^{2+} in $B220^+$ B cells were measured in real time with the use of a FACSVantage. The arrow shows addition of anti-IgM mAb. Representative results of three independent experiments are shown.

from the protein structure of sialoadhesin (27) and alignment of CD22 sequence with the sialoadhesin (28). These C′ and C″ β-strands are far away from the sialic acid-binding pocket of the Siglecs, which is formed by β-strands A, F and G (27). Therefore, the mutations present in these 'normal' forms of the CD22^a protein are unlikely to affect the sialic acid-binding site and to change the affinity of CD22 ligands.

In addition to the mutation mentioned above, *Cd22^a* also carries a short interspersed nucleotide element insertion in the second intron, leading to abnormal splicing of *Cd22^a* mRNA (21). Thus, aberrant CD22 molecules are likely expressed on *Cd22^a* B cells with substantial deletions in the first Ig-like domain which constitutes the ligand-binding site (21). Western blot analysis shows a slightly lower running CD22 protein in B cells from *Cd22^a* mice. This supports the possible expression of truncated isoforms of CD22, since the observed difference cannot be explained by a 6-amino-acid deletion present in the full-length CD22^a protein, as compared with the CD22^b protein (849 amino acids). Based on the sequence analysis on nine different aberrant CD22 mRNA species in *Cd22^a* mice (21), we expect that at least two isoforms (mCD22-VII and VIII) could express truncated forms of CD22, which have additional deletions of 34 and 62 amino acids. Notably, three others are likely to be unexpressed because of the presence of a premature stop codon. Since the relative abundance of these different CD22 mRNA transcripts has not been estimated, it is difficult to define the expression levels of aberrant CD22 proteins in relation to those of full-length CD22 protein. Clearly, further biochemical analysis is awaited to determine whether the majority of CD22 expressed in *Cd22^a* mice are indeed the truncated isoforms of CD22.

Possible expression of aberrant forms of CD22 likely impairs the binding of anti-CD22 CY34 mAb. The epitope for CY34 binding has been mapped to arginine at position 120 in the first Ig-like domain, in close vicinity to arginine at position 130, which is highly conserved within the Siglec family and required for sialic acid binding (28). Therefore, the ligand-binding capacity of the aberrant forms of CD22^a is likely to be affected. In addition, it should also be stressed that one of the truncated isoforms (mCD22-VII) possibly expressed in *Cd22^a* B cells lacks arginines at position 130 and 137 (21), which are involved in the ligand-binding activity (19). Thus, a decreased ability of the aberrant CD22^a proteins to bind to endogenous *cis* ligands could explain the higher degree of unmasked CD22 on the surface of B cells from *Cd22^a* mice that we observed in experiments using synthetic 2,6Sia-containing probe. Significantly, we also observed that sialidase-treated *Cd22^a* B cells displayed a more pronounced increase in binding of this probe, as compared with *Cd22^b* B cells. This could be due to the fact that more of the CD22^b protein is bound in *cis*, thus rendering the sialic acids on *Cd22^b* B cells less accessible to sialidase treatment than on their *Cd22^a* counterparts. However, it should be stressed that CD22^a efficiently binds this artificial ligand, probably because of a higher avidity of the synthetic ligand than of the endogenous *cis* ligands, due to its oligomeric structure.

Additionally, expression of CD22^a might affect homodimerization of CD22. Indeed, an N-linked potential glycosylation site is missing in the first Ig-like domain of CD22^a, due to the 6-amino-acid deletion present in the *Cd22^a* gene (23). In the CD22^b molecule, this glycosylation site may carry carbohydrates, including 2,6Sia, which can be sterically well accessible to the sialic acid-binding domain, also present in the first Ig-like domain. Indirect evidence for such a model of homodimerization comes from experiments in which sialylation of CD22 protein prevented CD22-mediated adhesion (29). Defective homodimerization could provide an alternative explanation why a higher fraction of CD22 is unbound in *cis*

on *Cd22*^{a} B cells, but more experiments are needed to test this possibility.

Impaired ligand binding by CD22 in *cis* on the B-cell surface has previously been shown to affect BCR signaling. When CD22 ligand binding was prevented by a genetic or pharmacological approach, anti-IgM-stimulated B cells showed less tyrosine phosphorylation of CD22, less SHP-1 recruitment and a higher Ca^{2+} mobilization (17, 18). However, a recently established CD22 knock-in mouse with a mutation in the ligand-binding domain of CD22 did not confirm these findings (19). In fact, we were unable to demonstrate significant differences in Ca^{2+} influx after anti-IgM stimulation of B cells between the various *Cd22*^{a} and *Cd22*^{b} mouse strains. Nevertheless, it should be stressed that B cells expressing a mutant CD22 lacking the ligand-binding domain displayed a phenotype of activated B cells, which is characterized by reduced IgM expression and augmented MHC class II expression, similar to that of CD22$^{-/-}$ B cells (3–6), and that CD22 ligand binding was involved in the regulation of BCR-mediated B-cell proliferation (19). Our analysis of B6 *Cd22* congenic mice revealed that *Cd22*^{a} B cells exhibit an activated phenotype (i.e. reduced surface IgM expression and increased surface MHC class II expression) similar to those of B cells expressing the mutant CD22. In view of the importance of CD22–CD22 ligand interaction in the regulation of B-cell activation, our data support the idea that the expression of the defective *Cd22*^{a} could contribute to enhanced B-cell activation, and thus favor the development of autoimmune responses in combination with other susceptibility alleles present in lupus-prone mice.

The expression of aberrant CD22 molecules in *Cd22*^{a} mice may have significant consequences for B-cell responses to antigen, and in particular for the spontaneous production of autoantibodies. A recent study suggested that simultaneous interactions between B cells and target cells via BCR–autoantigen and CD22–CD22 ligand could be a mechanism to prevent activation of potentially autoreactive B cells (30). Thus, in *Cd22*^{a} mice, lower basal expression levels and defective up-regulation of CD22 on potentially autoreactive B cells could favor the production of autoantibodies by reducing the BCR signaling threshold. In agreement, deficiency in CD22 expression, even at a heterozygous level, was able to promote the production of IgG anti-DNA autoantibodies in B6 mice (3, 21, 31). Interval mapping analysis for lupus susceptibility loci revealed that an NZW locus that peaked in the vicinity of the *Cd22*^{a} gene was strongly linked with autoantibody production and lupus-like glomerulonephritis (32–34). More recently, we have shown that B6 mice bearing an NZB chromosome 7 interval encompassing the *Cd22*^{a} gene spontaneously develop lupus-like autoimmune syndrome (24). Clearly, further assessment of the functional capacities of the different allelic forms of CD22 and of the regulation of CD22 expression will help to better understand the role of CD22 polymorphism in the development of B-cell-mediated autoimmune diseases.

Acknowledgements

We thank Mr Guy Brighouse and Mr Giuseppe Celetta for their excellent technical help. We thank the Consortium for Functional Glycomics for providing reagents. This work was supported by grants from the Swiss National Foundation for Scientific Research and the Deutsche Forschungsgemeinschaft.

Abbreviations

BCR	B-cell receptor
NeuGc-α2,6Gal–SAAP	*N*-glycolylneuramic acid–galactose–*N*-acetylglucosamine–streptavidin–alkaline phosphatase
SHP-1	SH-2 phosphotyrosine phosphatase
2,6Sia	α2,6-linked sialic acid
Siglec	sialic acid-binding Ig-like lectin
T1	transitional 1
TTBS-MP	TTBS containing 5% low-fat, dry milk powder

References

1 Nitschke, L. and Tsubata, L. 2004. Molecular interactions regulate BCR signal inhibition by CD22 and CD72. *Trends Immunol.* 25:543.
2 Doody, G. M., Justement, L. B., Delibrias, C. C. *et al.* 1995. A role in B cell activation for CD22 and the protein tyrosine phosphatase SHP. *Science* 269:242.
3 O'Keefe, T. L., Williams, G. T., Davies, S. L. and Neuberger, M. S. 1996. Hyperresponsive B cells in CD22-deficient mice. *Science* 274:798.
4 Otipoby, K. L., Andersson, K. B., Dravest, K. E. *et al.* 1996. CD22 regulates thymus-independent responses and the lifespan of B cells. *Nature* 384:634.
5 Sato, S., Miller, A. S., Inaoki, M. *et al.* 1996. CD22 is both a positive and negative regulator of B lymphocyte antigen receptor signal transduction: altered signaling in CD22-deficient mice. *Immunity* 5:551.
6 Nitschke, L., Carsetti, R., Ocker, B., Köhler, G. and Lamers, M. C. 1997. CD22 is a negative regulator of B-cell receptor signaling. *Curr. Biol.* 7:133.
7 Chen, J., McLean, P. A., Neel, B. G., Okunade, G., Shull, G. E. and Wortis, H. H. 2004. CD22 attenuates calcium signaling by potentiating plasma membrane calcium-ATPase activity. *Nat. Immunol.* 5:651.
8 Crocker, P. R. and Varki, A. 2001. Siglecs, sialic acids and innate immunity. *Trends Immunol.* 22:337.
9 Engel, P., Nojima, Y., Rothstein, D. *et al.* 1993. The same epitope on CD22 of B lymphocytes mediates the adhesion of erythrocytes, T and B lymphocytes, neutrophils, and monocytes. *J. Immunol.* 150:4719.
10 Hanasaki, K., Powell, L. D. and Varki, A. 1995. Binding of human plasma sialoglycoproteins by the B cell-specific lectin CD22. *J. Biol. Chem.* 270:7543.
11 Powell, L. D., Jain, R. K., Matta, K. L., Sabesan, S. and Varki, A. 1995. Characterization of sialyloligosaccharide binding by recombinant soluble and native cell-associated CD22. Evidence for a minimal structural recognition motif and the potential importance of multisite binding. *J. Biol. Chem.* 270:7523.
12 Kelm, S., Pelz, A., Schauer, R. *et al.* 1994. Sialoadhesin, myelin-associated glycoprotein and CD22 define a new family of sialic acid-dependent adhesion molecules of the immunoglobulin superfamily. *Curr. Biol.* 4:965.
13 Bakker, T. R., Piperi, C., Davies, E. A. and Merwe, P. A. 2002. Comparison of CD22 binding to native CD45 and synthetic oligosaccharide. *Eur. J. Immunol.* 32:1924.
14 Razi, N. and Varki, A. 1998. Masking and unmasking of the sialic acid-binding lectin activity of CD22 (Siglec-2) on B lymphocytes. *Proc. Natl Acad. Sci. USA* 95:7469.
15 Collins, B. E., Blixt, O., Bovin, N. V. *et al.* 2002. Constitutively unmasked CD22 on B cells of ST6Gal I knockout mice: novel sialoside probe for murine CD22. *Glycobiology* 12:563.
16 Danzer, C. P., Collins, B. E., Blixt, O., Paulson, J. C. and Nitschke, L. 2003. Transitional and marginal zone B cells have a high proportion of unmasked CD22: implications for BCR signaling. *Int. Immunol.* 15:1137.

17 Jin, L., McLean, P. A., Neel, B. G. and Wortis, H. H. 2002. Sialic acid binding domains of CD22 are required for negative regulation of B cell receptor signaling. *J. Exp. Med.* 195:1199.
18 Kelm, S., Gerlach, J., Brossmer, R., Danzer, C. P. and Nitschke, L. 2002. The ligand-binding domain of CD22 is needed for inhibition of the B cell receptor signaling, as demonstrated by a novel human CD22-specific inhibitor compound. *J. Exp. Med.* 195:1207.
19 Poe, J. C., Fujimoto, Y., Hasegawa, M. *et al.* 2004. CD22 regulates B lymphocyte function *in vivo* through both ligand-dependent and ligand-independent mechanisms. *Nat. Immunol.* 5:1078.
20 Torres, R. M., Law, C. L., Santos-Argumedo, L. *et al.* 1992. Identification and characterization of the murine homologue of CD22, a B lymphocyte-restricted adhesion molecule. *J. Immunol.* 149:2641.
21 Mary, C., Laporte, C., Parzy, D. *et al.* 2000. Dysregulated expression of the *Cd22* gene as a result of a short interspersed nucleotide element insertion in *Cd22*^{a} lupus-prone mice. *J. Immunol.* 165:2987.
22 Law, C. L., Aruffo, A., Chandran, K. A., Doty, R. T. and Clark, E. A. 1995. Ig domains 1 and 2 of murine CD22 constitute the ligand-binding domain and bind multiple sialylated ligands expressed on B and T cells. *J. Immunol.* 155:3368.
23 Lajaunias, F., Ibnou-Zekri, N., Fossati-Jimack, L. *et al.* 1999. Polymorphisms in the *Cd22* gene of inbred mouse strains. *Immunogenetics* 49:991.
24 Kikuchi, S., Fossati-Jimack, L., Moll, T. *et al.* 2005. Differential role of three major NZB-derived loci linked with *Yaa*-induced murine lupus nephritis. *J. Immunol.* 174:1111.
25 Symington, F. W., Subbarao, B., Mosier, D. E. and Sprent, J. 1982. Lyb-8.2: a new B cell antigen defined and characterized with a monoclonal antibody. *Immunogenetics* 16:381.
26 Hayakawa, K., Hardy, R. R., Parks, D. R. and Herzenberg, L. A. 1983. The "Ly-1 B" cell subpopulation in normal, immunodefective, and autoimmune mice. *J. Exp. Med.* 157:202.
27 May, A. P., Robinson, R. C., Vinson, M., Crocker, P. R. and Jones, E. Y. 1998. Crystal structure of the N-terminal domain of sialoadhesin in complex with 3′ sialyllactose at 1.85 Å resolution. *Mol. Cell* 1:719.
28 Van der Merwe, P. A., Crocker, P. R., Vinson, M., Barclay, A. N., Schauer, R. and Kelm, S. 1996. Localization of the putative sialic acid-binding site on the immunoglobulin superfamily cell-surface molecule CD22. *J. Biol. Chem.* 271:9273.
29 Braesch-Andersen, S. and Stamenkovic, I. 1994. Sialylation of the B lymphocyte molecule CD22 by α2,6-sialyltransferase is implicated in the regulation of CD22-mediated adhesion. *J. Biol. Chem.* 269:11783.
30 Lanoue, A., Batista, F. D., Stewart, M. and Neuberger, M. S. 2002. Interaction of CD22 with α2,6-linked sialoglycoconjugates: innate recognition of self to dampen B cell autoreactivity? *Eur. J. Immunol.* 32:348.
31 O'Keefe, T. L., Williams, G. T., Batista, F. D. and Neuberger, M. S. 1999. Deficiency in CD22, a B cell-specific inhibitory receptor, is sufficient to predispose to development of high affinity autoantibodies. *J. Exp. Med.* 189:1307.
32 Kono, D. H., Burlingame, R. W., Owens, D. G. *et al.* 1994. Lupus susceptibility loci in New Zealand mice. *Proc. Natl Acad. Sci. USA* 91:10168.
33 Morel, L., Rudofsky, U. H., Longmate, J. A., Schiffenbauer, J. and Wakeland, E. K. 1994. Polygenic control of susceptibility to murine systemic lupus erythematosus. *Immunity* 1:219.
34 Santiago, M. L., Mary, C., Parzy, D. *et al.* 1998. Linkage of a major quantitative trait locus to *Yaa* gene-induced lupus-like nephritis in (NZW × C57BL/6) F1 mice. *Eur. J. Immunol.* 28:4257.